AGE (2013) 35:1881–1897
DOI 10.1007/s11357-012-9491-x

Neuronal overexpression of insulin receptor substrate 2 leads to increased fat mass, insulin resistance, and glucose intolerance during aging

J. Zemva · M. Udelhoven · L. Moll · S. Freude · O. Stöhr · H. S. Brönneke · R. B. Drake · W. Krone · M. Schubert

Received: 20 May 2012 / Accepted: 5 November 2012 / Published online: 17 November 2012

Abstract The insulin receptor substrates (IRS) are adapter proteins mediating insulin's and IGF1's intracellular effects. Recent data suggest that IRS2 in the central nervous system (CNS) is involved in regulating fuel metabolism as well as memory formation. The present study aims to specifically define the role of chronically increased IRS2-mediated signal transduction in the CNS. We generated transgenic mice overexpressing IRS2 specifically in neurons (n*IRS2*^{tg}) and analyzed these in respect to energy metabolism, learning, and memory. Western blot (WB) analysis of n*IRS2*^{tg} brain lysates revealed increased IRS2 downstream signaling. Histopathological investigation of n*IRS2*^{tg} mice proved unaltered brain development and structure. Interestingly, n*IRS2*^{tg} mice showed decreased voluntary locomotoric activity during dark phase accompanied with decreased energy expenditure (EE) leading to increased fat mass. Accordingly, n*IRS2*^{tg} mice develop insulin resistance and glucose intolerance during aging. Exploratory behavior, motor function as well as food and water intake were unchanged in n*IRS2*^{tg} mice. Surprisingly, increased IRS2-mediated signals did not change spatial working memory in the T-maze task. Since FoxO1 is a key mediator of IRS2-transmitted signals, we additionally generated mice expressing a dominant negative mutant of *FoxO1* (*FoxO1DN*) specifically in neurons. This mutant mimics the effect of increased IRS2

Electronic supplementary material The online version of this article (doi:10.1007/s11357-012-9491-x) contains supplementary material, which is available to authorized users.

J. Zemva and M. Udelhoven contributed equally to this study.

J. Zemva · M. Udelhoven · L. Moll · S. Freude · O. Stöhr · R. B. Drake · W. Krone · M. Schubert (✉)
Center for Endocrinology, Diabetes and Preventive Medicine (CEDP), University of Cologne,
Kerpener Str. 62,
50937 Cologne, Germany
e-mail: markus.schubert@uni-koeln.de

J. Zemva · M. Udelhoven · L. Moll · S. Freude · O. Stöhr · R. B. Drake · W. Krone · M. Schubert
Center for Molecular Medicine Cologne (CMMC), University of Cologne,
Robert-Koch-Str. 21,
50931 Cologne, Germany

H. S. Brönneke · W. Krone · M. Schubert
Cologne Cluster of Excellence in Cellular Stress Responses in Aging-associated Diseases (CECAD), University of Cologne,
Cologne, Germany

L. Moll
Biochemistry and Molecular Biology, Institute for Molecular Research Israel—Canada (IMRIC), School of Medicine of the Hebrew University of Jerusalem,
Jerusalem 91120, Israel

signaling on FoxO-mediated transcription. Interestingly, the phenotype observed in n*IRS2*^{tg} mice was not present in *FoxO1DN* mice. Therefore, increased neuronal IRS2 signaling causes decreased locomotoric activity in the presence of unaltered exploratory behavior and motor coordination that might lead to increased fat mass, insulin resistance, and glucose intolerance during aging independent of FoxO1-mediated transcription.

Keywords IRS2 · Brain · Mice · Insulin resistance · Diabetes · Locomotoric activity

Introduction

Insulin receptor substrate (IRS) proteins integrate signals from the insulin and IGF1 receptor with those generated by proinflammatory cytokines, nutrients, and neurotrophins (Udelhoven et al. 2010a, b; Yamada et al. 1997; Yenush and White 1997). Phosphorylated IRS proteins activate multiple signaling pathways, including the PI3K and Erk cascades (Dong et al. 2008; Saltiel and Kahn 2001; Withers et al. 1999). There are at least four members of the IRS protein family known, namely, IRS1–4. IRS1 and IRS2 are expressed throughout the brain. The expression of IRS4 is restricted to the hypothalamus, and IRS3 has not been described in the murine brain so far (Lavan et al. 1997a, b; Sun et al. 1991; Sun et al. 1995).

Activation of the PI3K pathway promotes cell growth and survival by phosphorylating FoxO transcription factors to regulate gene transcription and Bcl2-associated death protein to inhibit apoptosis (Brunet et al. 1999; Stohr et al. 2011a, b). Akt inactivates GSK3β, affecting cellular metabolism, proliferation, and survival (Cheng and White 2012; White 2003). The IRS2 branch of the insulin/IGF1 signaling cascade controls hepatic insulin response as well as pancreatic β cell growth and function (Burks et al. 2000; Cheng et al. 2009; Withers et al. 1999).

However, the role of IRS2 in the central nervous system (CNS) is controversially discussed (Selman et al. 2008). Earlier studies have shown that the IRS2 branch of the IR/IGF1R signaling cascade regulates neuronal proliferation (Schubert et al. 2003), apoptosis (Chirivella et al. 2012), and timing of myelination (Freude et al. 2008). Surprisingly, deletion of IRS2 specifically in the brain increases lifespan in the presence of peripheral insulin resistance (Taguchi et al. 2007).

Furthermore, IRS2 has been linked to the pathogenesis of neurodegenerative diseases, e.g., Alzheimer's disease (AD) (Freude et al. 2009a, b; Moloney et al. 2010) and Huntington's disease (Sadagurski et al. 2011). The abundance of IRS2 in AD patients is dramatically reduced, suggesting a role of IRS2-mediated signals in the pathogenesis of AD (Moloney et al. 2010). Accordingly, intranasal applied insulin has been used as therapeutic approach to improve memory formation (Craft et al. 2012; Dhamoon et al. 2009). Studies in humans up to 6 months suggest beneficial effects of intranasal insulin application on memory formation (Craft et al. 2012) and the development of obesity in men (Hallschmid et al. 2004). However, long-term studies in transgenic mouse models are less optimistic (Freude et al. 2009a, b). Data obtained from mice with brain-specific IRS2 deletion suggest that IRS2 is a negative regulator of memory formation possibly via modulating dendritic spine density (Irvine et al. 2011). Furthermore, deletion of IRS2 might have beneficial effects on amyloid pathology of AD mouse models (Cohen et al. 2009; Freude et al. 2009a, b; Killick et al. 2009). Thus, reduced IRS2-mediated signaling in the CNS has been linked to increased lifespan, decreased proteotoxicity in AD and Huntigton's disease, increased memory formation, and also increased insulin resistance.

However, there are no data available exploring the long-term effects of increased IRS2 signaling in the CNS. Therefore, we generated mice overexpressing IRS2 in postmitotic neurons and studied these mice up to 100 weeks of age. Here, we show that increased neuron-specific IRS2 signaling in mice decreases locomotor activity in the presence of unaltered exploratory behavior and motor function leading to increased fat mass, insulin resistance, and glucose intolerance during aging.

Materials and methods

Generation of nIRS2^{tg} mice: cloning of targeting vector

pBluescript KS II *FLAG-mIRS2* was serially cut with *Not*I and *Hin*dIII. A self-pairing, double-stranded 5′-phosphorylated linker was inserted into both restriction sites adding a *Mlu*I site at the beginning (5′-GGCCGAACGCGTTC-3′) and at the end (5′-AGCTAACGCGTT-3′) of the open reading frame. Afterwards, *FLAG-mIRS2* was harvested using *Mlu*I

and ligated into pCAGGS *ROSA26* vector using an *Asi*I restriction site. After sequence verification, plasmid DNA was amplified and used for ES cell transfection.

Cell culture

Embryonic fibroblasts (EF) were cultured in high glucose (4.5 g/l), Dulbecco's Modified Eagle's Medium (DMEM) GlutaMax (Invitrogen) containing 1 mM sodium pyruvate (Invitrogen), and 10 % fetal calf serum (FCS) (Biochrom). Feeder layer EF were generated as described previously (Kuhn and Torres 2002).

Embryonic stem cell transfection

pCAGGS *FLAG-mIRS2* was linearized. Fifty micrograms of DNA was precipitated with ethanol and resuspended in 400 μl cell culture medium RPMI-1640. In parallel, ~1×10^7 V6.5 ES (129SV×C57BL/6, F1 Hybrid) (Eggan et al. 2001) were resuspended in 400 μl RPMI on ice. Both samples were mixed slightly and transferred into an electroporation cuvette (0.4 cm). Electroporation was performed using a gene pulser (BioRad) with a 500 μF, 240 V pulse. Afterwards, cells were chilled on ice for 5 min (Kuhn and Torres 2002). One electroporation sample was split into four 10-cm cell culture dishes containing an EF layer. For selection, cells were treated with 250 μg/ml G418 48 h after transfection. Seven days after selection, resistant colonies were picked and transferred into 96-well cell culture plates containing an EF layer. Positive clones identified in southern blot (SB) experiments were thawed and reseeded on an EF feeder layer in cell culture plates. After a second confirmation via SB, a positive clone was used for further expansion. Finally, microinjection into blastocytes and embryo transfer into pseudopregnant mice were carried out in the Centre for Mouse Genetics, University of Cologne.

Southern blotting

Cells were lysed in 96-well cell culture plates with lysis buffer (10 mM Tris/HCl pH 7.5, 10 mM Ethylenediaminetetraacetic acid (EDTA), 10 mM NaCl, 0.5 % (w/v) lauroylsarcosine) containing 0.5 mg/ml proteinase K at 56 °C overnight. Afterwards, genomic DNA was precipitated with isopropanol and washed with 70 % (v/v) ethanol. After digesting with *Eco*RI over 4 days at 37 °C, 10 μg DNA was separated on an agarose gel. Subsequently, DNA was transferred to a Hybond nylon membrane (Amersham) and was fixed by baking. For hybridization, an α-^{32}P-dCTP-phosphorylated *ROSA26* probe (1,200-bp *Eco*RI/*Bam*HI fragment from A-04 plasmid) (Mao et al. 1999) and a neomycin probe (forward TGAATGAACTGCAGGACGAGG, reverse GCCGCCAAGCTCTTCAGCAATAT, polymerase chain reaction (PCR) on pBluescript-neo-TK) were used. Labeled probes were generated using the random prime-based Ladderman™ Labeling Kit (Takara) following manufacturer's instructions. For hybridization, Hybond nylon membranes were incubated with probes at 65 °C overnight. Afterwards, membranes were washed with saline-sodium citrate (SSC) buffer at 68 °C for 20 min. Finally, membranes were analyzed using a BAS 1000 Phosphoimager (Fujifilm).

Genotyping

Mice were genotyped via PCR using genomic DNA isolated from tail tips. Primers were used as following: *FLAG* forward 5′-GACTACAAAGATGACGACGATAA-3′, *IRS2* reverse 5′-GGTGTAGTGGGCGATCAGGTACTTGTG-3′, *ROSA26* forward 5′-AAGGGAGCTGCAGTGGAGTAGGCGGGGAGAAGG-3′, and *ROSA26* reverse 5′-GGATATGAAGTACTGGGCTCTTTAAA-3′. GoTaq Polymerase (Promega) was used for PCR as described in the manufacturer's instructions.

SynCre mice were genotyped as described previously (Freude et al. 2009a, b) and crossed with IRS2^{tg} to achieve neuron-specific deletion (n*IRS2*^{tg} mice). Wild type (WT) mice served as controls. In order to exclude artifacts due to estrous cycle, we only used male mice on a C57BL/6N background. Animals were housed in a 12-h light–dark cycle (07:00 on, 19:00 off) and were fed a standard rodent diet (Cat. N. TPF-1314, Altromin, Lage, Germany: 89 % dry matter, 22.5 % crude protein, 5 % crude fat, 4.5 % crude fiber, 6.5 % crude ash, 50.5 % nitrogen free extracts, and a standard amount of different minerals, amino acids, vitamins, and trace elements).

FoxO1DN mice

FoxO1DN mice were generated as described previously (Stohr et al. 2011a, b). Similar to the IRS2^{tg} construct,

FoxO1DN cDNA was cloned into the *ROSA26locus*. Again, to achieve neuron-specific expression, *FoxO1DN* mice were crossed with SynCre mice. All animal experiments were performed in accordance with the principles of laboratory animal care of the National Institute of Health (NIH) as well as the German Laws for Animal Protection and approved by the local animal care committee and the Bezirks- regierung Köln.

Metabolic characterization, body composition, glucose/insulin tolerance tests, and ELISA

Body fat content was measured in vivo by nuclear magnetic resonance (NMR) using a minispec mq7.5 (Bruker Optik, Ettlingen, Germany) as previously described (Mesaros et al. 2008). Glucose and insulin tolerance tests were performed as described previously (Freude et al. 2012; Stohr et al. 2011a, b). Results are shown as blood glucose concentration (milligram per deciliter) for glucose tolerance tests (GTTs) and as percentage of initial blood glucose concentration for insulin tolerance tests (ITT).

Serum was collected from mice at the age of 40 weeks. Leptin and adiponectin were measured as described in the according protocol (Mouse/Rat Leptin Enzyme Linked Immunosorbent Assay (ELISA) [E06], Mouse adiponectin ELISA [E091M], Mediagnost, Reutlingen, Germany).

Indirect calorimetry and physical activity measurement

Mice were measured in an open circuit calorimetry system (PhenoMaster, TSE Systems GmbH, Bad Homburg, Germany). Measurements were made as described previously according to the guidelines suggested by Tschop et al. (2012). The following parameters were obtained: energy expenditure (EE), respiratory quotient (RQ), home cage activity, food intake, water intake, CO_2 production, and O_2 consumption. Presented data are average values obtained in these recordings (at least 48 h).

Anxiety behavior, motor functioning, and spatial working memory

Elevated O-maze test was performed as described previously (Freude et al. 2012). Time spent in the open/closed sections was evaluated.

Open field tests were carried out as described previously (Konner et al. 2011). Time spent in the central part (25 cm×25 cm) versus time spent at the border was evaluated. Rotarod test was performed as described previously (Freude et al. 2008). The latency [s] to fall from the rod was recorded.

The T-maze test was used to assess functioning of the hippocampus. We used an enclosed T-maze which had the following dimensions: start alley and goal arms, 30 cm×10 cm and wall height, 20 cm. The T-maze had a conventional design with one guillotine door at the end of the start alley and one at the beginning of each goal arm. Spontaneous alternation was tested as described by Deacon and Rawlins (2006). Seven trials per mouse were carried out and trials were run over several days.

Immunoblotting

Protein expression from hippocampal and cortical brain lysates (100 μg) was determined as previously described (Stohr et al. 2011a, b; Zemva and Schubert 2011; Zemva et al. 2012). The following primary antibodies were used: anti-β-subunit of IR, anti-IGF1R, anti-Akt, anti-phospho-Akt (Ser473), anti-IRS1, anti-IRS2, anti-FoxO1, anti-FoxO3a, anti-enhanced green fluorescent protein (GFP) (Cell Signaling Technology, Inc, MA, USA), and anti-actin (Santa Cruz, CA, USA; MP Biomedicals Europe, France). The secondary anti-rabbit/mouse-IgG were purchased from Sigma-Aldrich, Munich, Germany.

Fig. 1 Generation of *FLAG-IRS2*^{tg} mice and conformation of transgene expression. **a** Schematic drawing of the *ROSA26-IRS2*-targeting vector before and after homologous recombination (*filled triangles* loxP sites, *closed ellipses* FRT sites, *filled rectangles* exons). Sites of specific primers for genotyping PCR are indicated. **b** EcoRI-digested genomic DNA derived from ES used for microinjection tested in Southern blot experiments. *Left panel ROSA26* probe results in a 7.1-kb band and a 16-kb wild type (WT) band. *Right panel* Hybridization with internal neomycin probe presents with a 7.1-kb band in transgene cells. **c** PCR using genomic DNA derived from mouse tail biopsies: single 600-bp band (WT), double band (400 bp, 600 bp) (heterozygous *IRS2*^{tg} mice). **d** Western blot of hippocampal and cortical lysates using GFP antibodies. Actin served as loading control. **e** GFP immunohistochemistry of hippocampi of adult n*IRS2*^{tg} and WT mice. *Upper panel* hippocampal formation; *lower panel* cortical sections. *SA* adenoviral splice acceptor, *CAG* chicken β-actin promoter with upstream CMV enhancer, *Neo*^{R} neomycin resistance, *WSS* Westphal stop sequence, *IRES* internal ribosomal entry site, *GFP* enhanced green fluorescent protein, *DTA* diphtheria toxin A. **e** *Upper panel*: magnification: 20×; *lower panel*: magnification: 60×

Immunohistochemistry

Brain tissue was bedded in Tissue-Tek® O.C.T. Compound™ (Sakura Finetek Europe, Leiden, Netherlands) and cut into 20-µm slices. Slices were fixated and preincubated with 5 % goat serum (Vectastain, Burlingame, CA, USA). Primary antibodies were used against GFP (Invitrogen, Life Technologies Ltd., Paisley, UK) and glial fibrillary acidic protein (GFAP) (DakoCytomation, Glostrup,

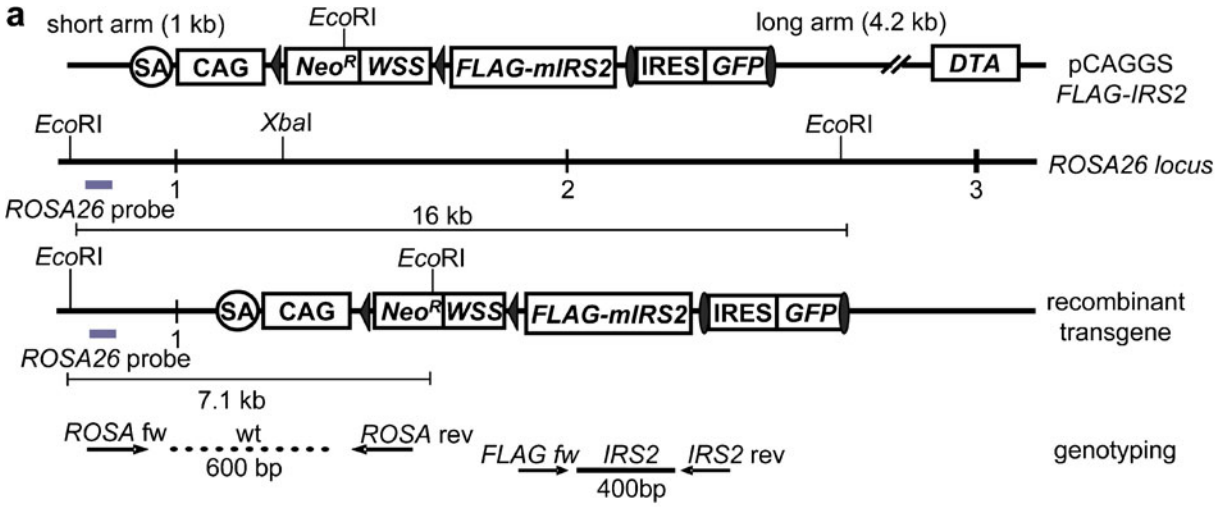

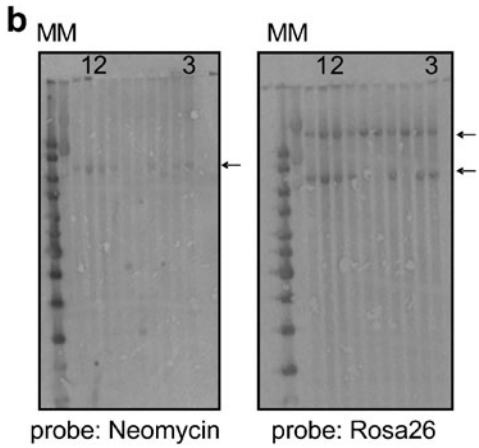

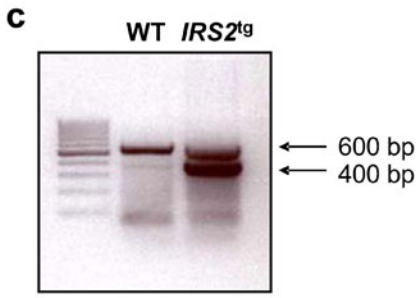

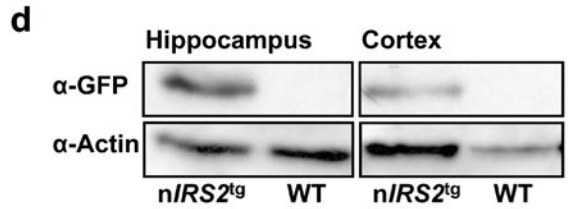

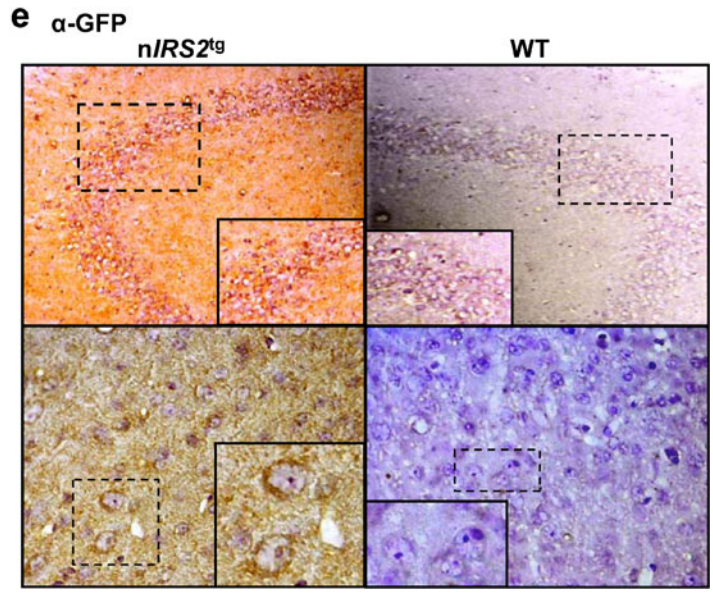

Denmark). Biotinylated secondary antibodies and ABC kits were purchased from Vectastain (Vectastain Elite Kit Standard/Rabbit) and used following manufacturer's instructions. Diaminobenzidine served as substrate and hemalm as counter stain.

Statistical analysis

For statistical analysis of the different study groups, unpaired Student's *t* test was performed. Statistical significance was defined as $^{*}p<0.05$.

Results

Generation of nIRS2^{tg} mice

To generate mice overexpressing tagged mIRS2, we ligated *FLAG-mIRS2* derived from pBluescript KS II *FLAG-mIRS2* into the pCAGGS vector. Additionally, the *FLAG-mIRS2* construct harbors a loxP site flanked Westphal stop cassette and a FRT site-framed *IRES-eGFP* cassette in order to identify transgene expressing cells in vivo (Fig. 1a). The final construct, pCAGGS *FLAG-mIRS2*, was used as targeting vector (Fig. 1a). The construct was linearized and transfected in V6.5 ES as described in the "Materials and methods". Only stem cells integrating the targeting vector via homologous recombination survived, since stem cells that integrated the targeting construct randomly died because of constitutive expression of diphtheria toxin (Fig. 1a). One hundred clones were tested using SB for correct integration of the construct. Prior to SB, DNA was digested using *Eco*RI leading to a 16-kb band in WT and 16-kb and 7.1-kb bands in transgenic cells using the appropriate *ROSA26* probe (Fig. 1b). To verify single integration, a neomycin probe was used. A 7.1-kb band proves insertion of the transgene (Fig. 1b). Positive clones were selected for microinjection in blastocysts and embryos were implanted as described in "Materials and methods". Finally, chimeric mice were backcrossed with C57BL/6N mice for eight generations. Additionally, we performed PCR using genomic DNA derived from mouse tail biopsies to identify the transgene. Specific primers were used to identify the FLAG-tagged *mIRS2* transgene (Fig. 1c). As control, a 600-bp fragment was generated in WT and heterozygous transgene mice using *ROSA26* forward and reverse primers (Fig. 1a, c). In order to achieve neuron-specific expression, mice transgenically expressing the Cre-recombinase under control of the synapsin-1 promoter (SynCre mice)

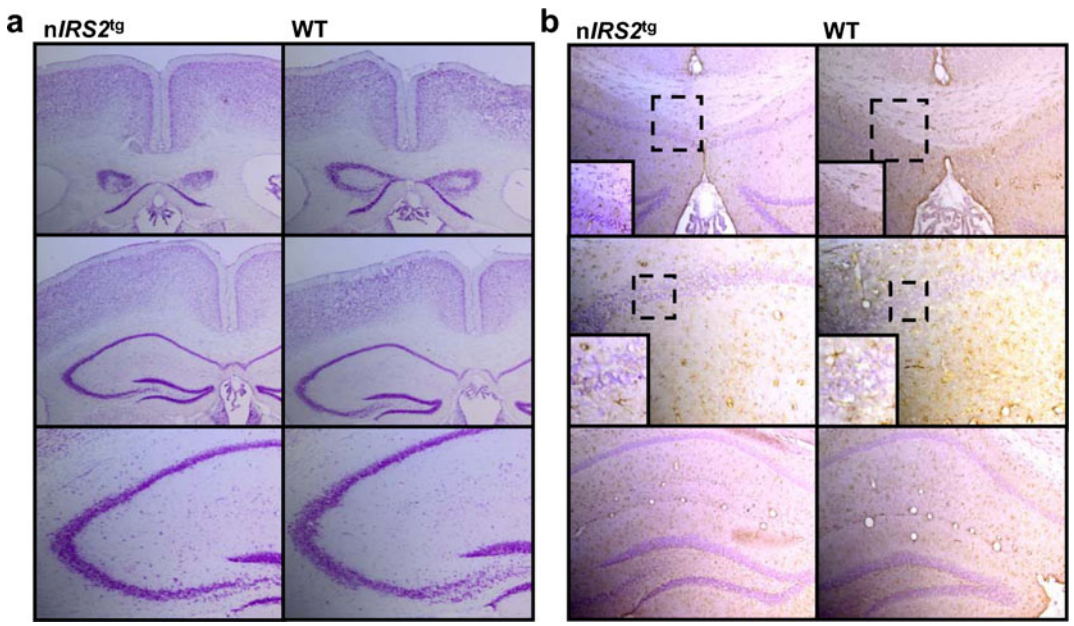

Fig. 2 Histological analysis of n*IRS2*^{tg} mice. **a** Nissl staining of hippocampal formation of adult n*IRS2*^{tg} and wild type (WT) mice. **b** Glial fibrillary acidic protein (GFAP) immunohistochemistry of hippocampal sections of adult n*IRS2*^{tg} and WT mice. (*Upper and lower image*: magnification 10×; *central image*: magnification 20×)

were used as described previously (Zhu et al. 2001). We and others have crossed SynCre mice with lacZ reporter mice. These experiments revealed strong Cre-recombinase expression in the hippocampus (dentate gyrus, CA2/3(1)) and, to a lesser extent, in the cortical regions (largely restricted to the lower boundary of layer IV), piriform cortex, amygdala, thalamus, hypothalamus (including the arcuate nucleus), and the brainstem (Freude et al. 2009a, b; He et al. 2004; Zhu et al. 2001) (data not shown). Accordingly, GFP expression was strongly detectable via Western blot (WB) in lysates of isolated hippocampi and, to a lesser extent, in cortex (Fig. 1d). Using GFP immunohistochemistry, we could confirm transgene expression in the above described regions (e.g., Fig. 1e, CA2/3(1) and layer IV neurons of the frontal cortex).

Histological analysis of male nIRS2^{tg} mice

Appropriate development of the CNS depends on the balance and timing of proliferation, apoptosis, and cell migration (Schubert et al. 2003). Since IRS2 has been linked to neuronal proliferation and apoptosis during development, we investigated serial sections through brains of adult WT and n*IRS2*^{tg} mice. Nissl staining revealed no alterations of brain structure (Fig. 2a). Furthermore, we used GFAP staining to detect activated astrocytes as an unspecific marker for neuronal damage. However, staining intensity and pattern were similar in WT and n*IRS2*^{tg} mice (Fig. 2b). Thus, n*IRS2*^{tg} have normal brain structure without any signs of neuronal damage or loss.

IRS2-mediated signaling in the CNS of nIRS2^{tg} mice

After having shown that n*IRS2*^{tg} mice indeed express *GFP* as part of the *mIRS2* transgene, we next aimed to show whether these mice show altered IRS2 expression or IRS2-mediated signaling in the CNS. At first, we investigated IRS2 expression from hippocampal and cortical lysates. As suggested by the GFP WB and the immunohistochemistry from n*IRS2*^{tg} and WT

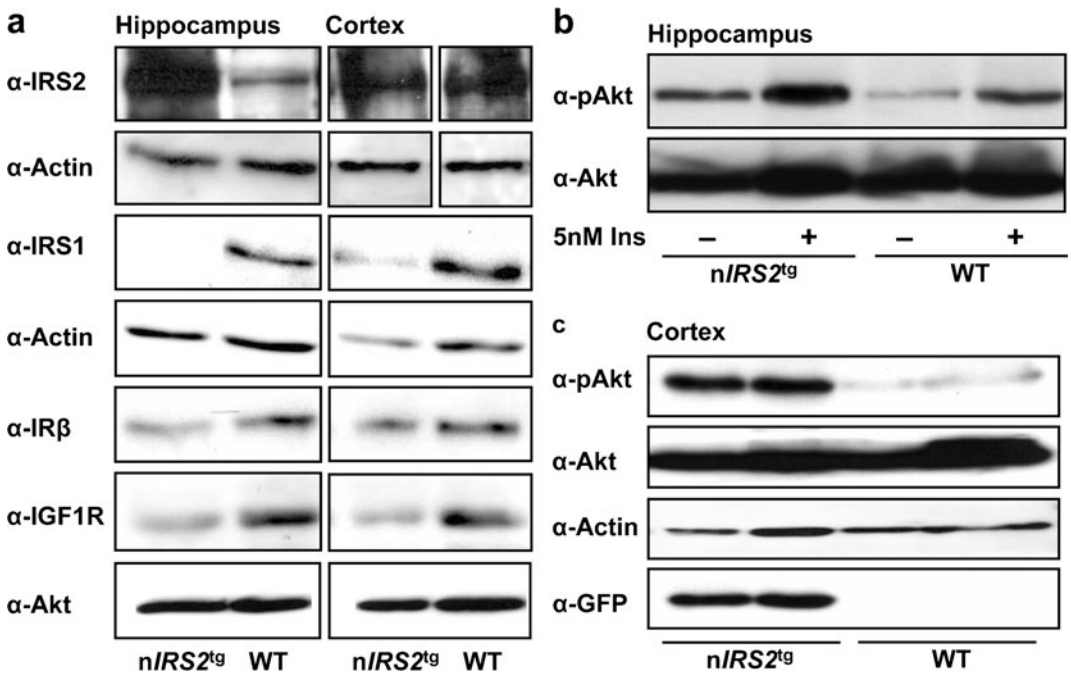

Fig. 3 IRS2-mediated signals in hippocampus and cortex of male n*IRS2*^{tg} mice. **a** Western blots (WB) of hippocampal and cortical lysates of adult n*IRS2*^{tg} and WT mice using antibodies against IRS2, IRS1, IRβ, and IGF1R. Actin and Akt served as loading controls. **b** WB analysis after ex vivo stimulation with 5 nM insulin of hippocampi of adult n*IRS2*^{tg} and WT mice using antibodies against phospho-Akt (Ser473), and Akt served as loading control. **c** WB of cortical lysates using antibodies against phospho-Akt (Ser473), Akt, and GFP. Actin served as loading control. Individual bands of the WB represent individual animals (3 independent experiments). *IRS2* insulin receptor substrate 2, *IRS1* insulin receptor substrate 1, *IRβ* beta-subunit of insulin receptor, *IGF1R* insulinlike growth factor 1 receptor, *Akt* protein kinase B, *GFP* green fluorescent protein

brains, IRS2 was largely overexpressed in the hippocampus and, to a lesser extent, in the cortex (Fig. 3a). Thus, we generated a mouse model overexpressing IRS2 predominantly in the hippocampus. Interestingly, IRS1 was slightly downregulated in the hippocampus and cortex of n*IRS2*^{tg} compared to WT mice (Fig. 3a), suggesting a compensatory mechanism. Accordingly, we observed a reduced expression of the IR and IGF1R in hippocampal and cortical lysates in 50 % of the animals (Fig. 3a). We then addressed the question whether increased IRS2 abundance indeed influences downstream signaling. WB of isolated hippocampi revealed increased basal- and insulin-stimulated Akt phosphorylation at Ser473 (Fig. 3b). Furthermore, basal AktSer473 phosphorylation was upregulated in the cortex of n*IRS2*^{tg} compared to WT mice (Fig. 3c). Similar results were obtained for phosphorylation of Erk1/2 at Thr202 and Tyr204 (data not shown). Thus, even though overexpression of IRS2 might lead to compensatory downregulation of IR/IGF1R or IRS1, downstream activity of the MAPK and PI3K pathways is increased in n*IRS2*^{tg} compared to WT mice.

Increased fat mass in male nIRS2^{tg} mice

Central IRS2 signaling has been linked to the regulation of fuel metabolism and insulin sensitivity. Interestingly, mice heterozygous or homozygous for our transgene appear to gain more abdominal fat mass during aging (Suppl. Fig. 1). Accordingly, we investigated body composition and glucose metabolism in n*IRS2*^{tg} mice. NMR analysis of n*IRS2*^{tg} males revealed significantly increased fat mass compared to male WT littermates (Fig. 4a). Consistently, leptin levels were higher in n*IRS2*^{tg} males but failed to reach significance because of large SD (n=6, p=0.08,

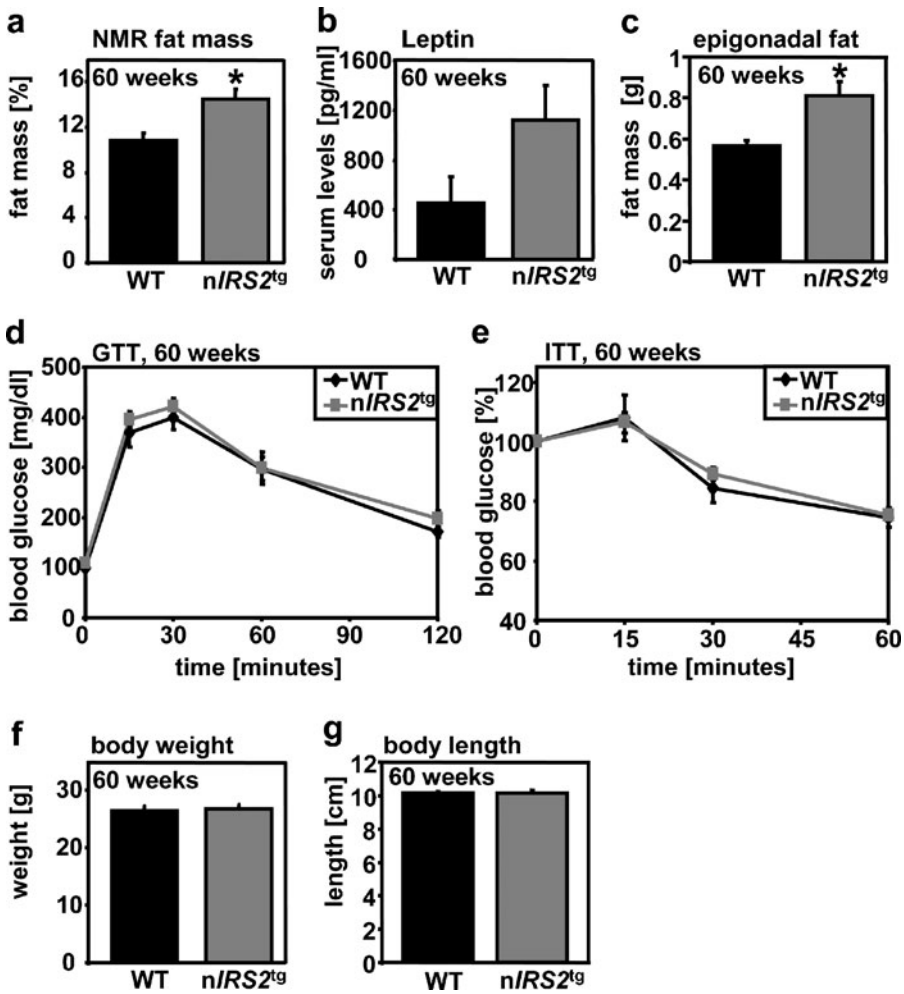

Fig. 4 Increased fat mass in male n*IRS2*^{tg} mice and respective controls. **a** Fat mass measured by nuclear magnetic resonance (NMR). **b** ELISA analysis of leptin. **c** Epigonadal fat mass. **d**–**e** Glucose (GTT) and insulin (ITT) tolerance tests. **f**–**g** Body weight and length. Data are expressed as means ± SEM, n=6 per group, $^{*}p<0.05$ (Student's t test), **a**–**g**: age 60 weeks

Fig. 4b) and epigonadal fat pads were significantly enlarged in n*IRS2*^{tg} mice (Fig. 4c). Adiponectin levels remained unchanged (data not shown). Glucose metabolism was nearly unaltered in male n*IRS2*^{tg} mice as determined by GTT (Fig. 4d) and ITT (Fig. 4e) at 60 weeks of age. Furthermore, body weight and body length (Fig. 4f, g) as well as organ weights (brain, liver, heart, kidney, spleen, lung, and testes; data not shown) were undistinguishable between the two genotypes. Thus, increased IRS2-mediated signals in neurons increase body fat mass but do not significantly influence body growth.

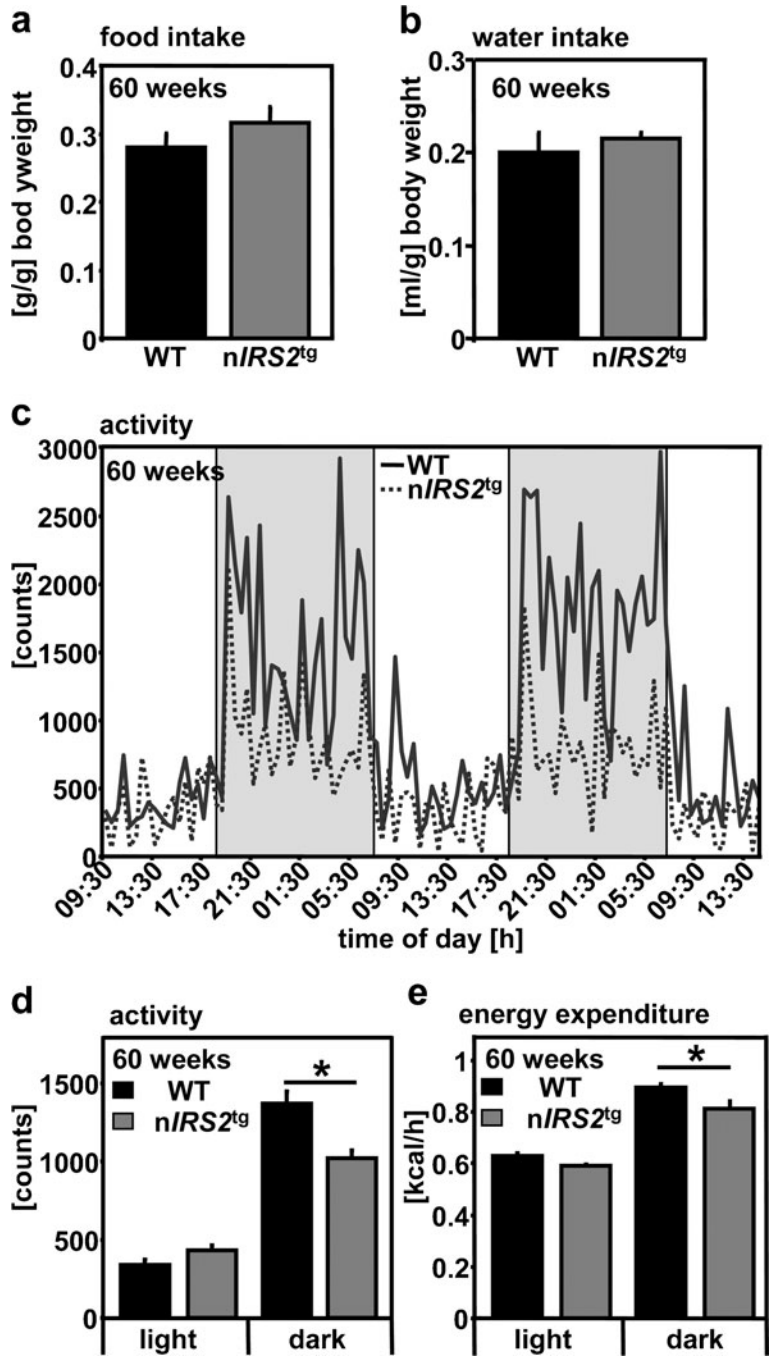

Fig. 5 Locomotor activity and energy expenditure of male n*IRS2*^{tg} mice and respective controls. **a**–**b** Food and water intake per gram of body weight. **c**–**d** Voluntary locomotor activity and circadian pattern. **e** Energy expenditure. Data represent means ± SEM, $n=6$ per group, $^{*}p<0.05$ (Student's t test), age: 60 weeks

Voluntary locomotor activity and EE in male nIRS2^{tg} mice

In order to analyze the physiological basis for the increased fat mass in n*IRS2*^{tg} males, we measured food and water intake, locomotor activity, and EE. Interestingly, food and water intake was not different in n*IRS2*^{tg} males compared to WT littermates (Fig. 5a, b). Consequently, we analyzed voluntary locomotor activity in our mice revealing significantly decreased activity in n*IRS2*^{tg} males during dark phase (Fig. 5c, d). However, circadian pattern of locomotor activity was unchanged (Fig. 5c). Accordingly, EE during dark phase was significantly decreased in n*IRS2*^{tg} males compared to WT mice within the expected range (Fig. 5e). The difference in EE during dark phase remained significant when normalizing the data to body weight (data not show).

Exploratory behavior and motor coordination in male nIRS2^{tg} mice

Since alterations of exploratory behavior or motor coordination might influence voluntary activity, we used the elevated O-maze test, open field test, and rotarod task to comprehensively analyze our mice. However, we did not observe any differences between male n*IRS2*^{tg} and WT littermates using these tests (Suppl. Fig. 2a–c). Thus, n*IRS2*^{tg} males show decreased locomotor activity accompanied by reduced EE during dark phase in the presence of unaltered exploratory behavior or motor coordination.

Glucose intolerance and insulin resistance in 100-week-old male nIRS2^{tg} mice

In order to answer the question whether the alterations in fat mass and activity might have metabolic conse-

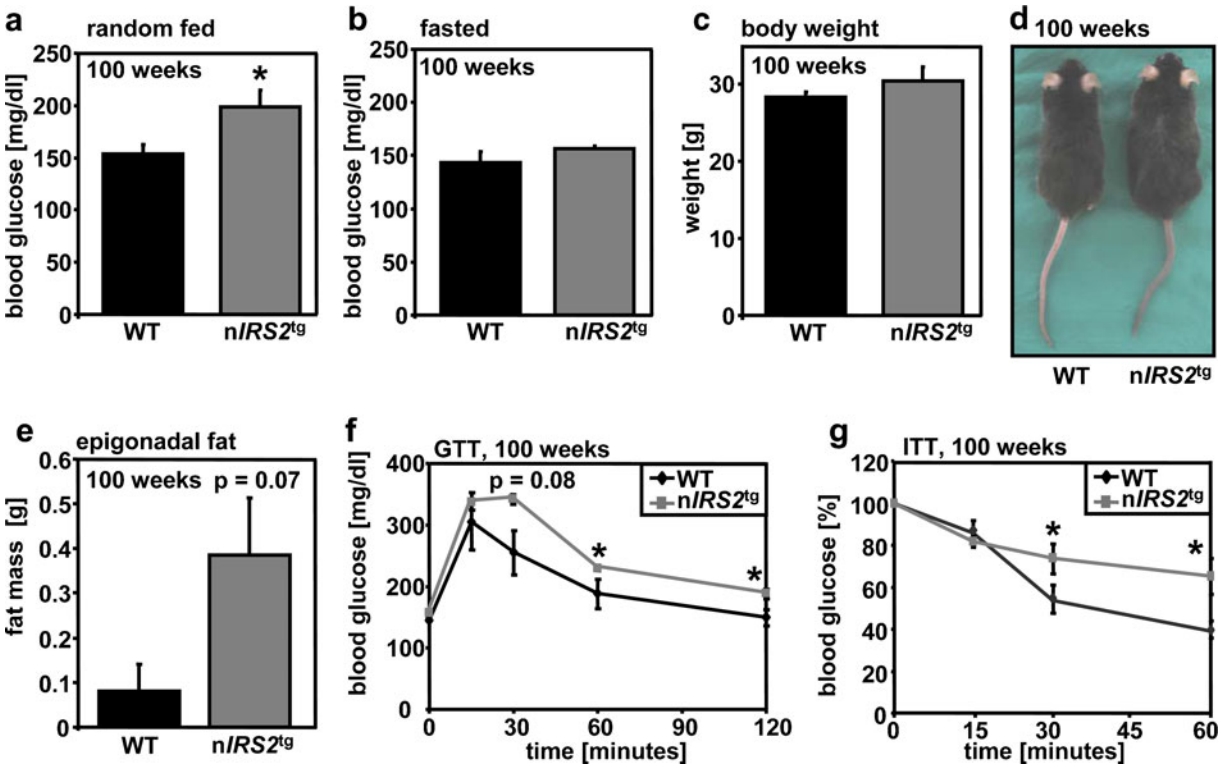

Fig. 6 Glucose intolerance and insulin resistance in 100-week-old male n*IRS2*^{tg} mice and respective controls. **a**–**b** Random fed and fasting blood glucose levels. **c**–**e** Body weight and epigonadal fat mass. **f**–**g** Glucose (GTT) and insulin (ITT) tolerance tests. Data shown as means ± SEM, n=6 per group, $^{*}p<0.05$ (Student's t test), age: 100 weeks

quences in older age, we investigated n*IRS2*^{tg} males at 100 weeks of age. Interestingly, these mice had significantly increased random-fed blood glucose levels (Fig. 6a), whereas fasted blood glucose concentrations remained unchanged (Fig. 6b). Body weight of n*IRS2*^{tg} was slightly but not significantly higher (Fig. 6c). Animals looked healthy with slightly more pronounced waist (Fig. 6d). Epigonadal fat pads were still enlarged in n*IRS2*^{tg} males compared to WT mice. However, due to large SD, this difference did not reach significance (n=6, p=0.07, Fig. 6e). Interestingly, GTT (Fig. 6f) and ITT (Fig. 6g) revealed significant differences between the genotypes at 100 weeks of age. Male n*IRS2*^{tg} mice were glucose intolerant and significantly more insulin resistant than WT males. Thus, n*IRS2*^{tg} mice develop insulin resistance and glucose intolerance during aging.

Spatial working memory in male nIRS2^{tg} mice

Recently published data suggest that IRS2 might be a negative regulator for learning and memory (Irvine et al. 2011). In particular, mice deficient for IRS2 in all CNS cells from early development on including astrocytes, oligodenrocytes, and neurons show increased spatial working memory in the T-maze test (spontaneous alterations). Therefore, we tested 20-week- and 100-week-old animals in this test. However, we did not observe any significant difference between the genotypes (Suppl. Fig. 3a). Hence, we can exclude severe impairment of spatial working memory in male n*IRS2*^{tg} mice.

Characterization of FoxO1DN mice

FoxO1, as downstream target of IRS2-mediated signals, has been shown to mediate several metabolic effects observed in IRS2-deficient mouse models. IRS2 signaling leads to phosphorylation of FoxO1 via Akt inducing its nuclear export and degradation. Therefore, IRS2 is a negative regulator of FoxO1-mediated transcription. To mimic inhibition of FoxO1-mediated transcription, we generated a transactivation domain-deleted FoxO1 mutant (Fig. 7a) to suppress FoxO1-induced transcription (FoxO1DN). Our approach to inhibit FoxO1-mediated transcription using the FoxO1DN mutant has been described previously and is well characterized (Kitamura et al. 2007).

To further explore the molecular mechanism of the phenotype of n*IRS2*^{tg} mice, we analyzed mice expressing this dominant negative FoxO1 variant specifically in neurons. We generated these mice using a similar targeting strategy as described above for the n*IRS2*^{tg} mice (Stohr et al. 2011a, b). To express Cre-recombinase, we

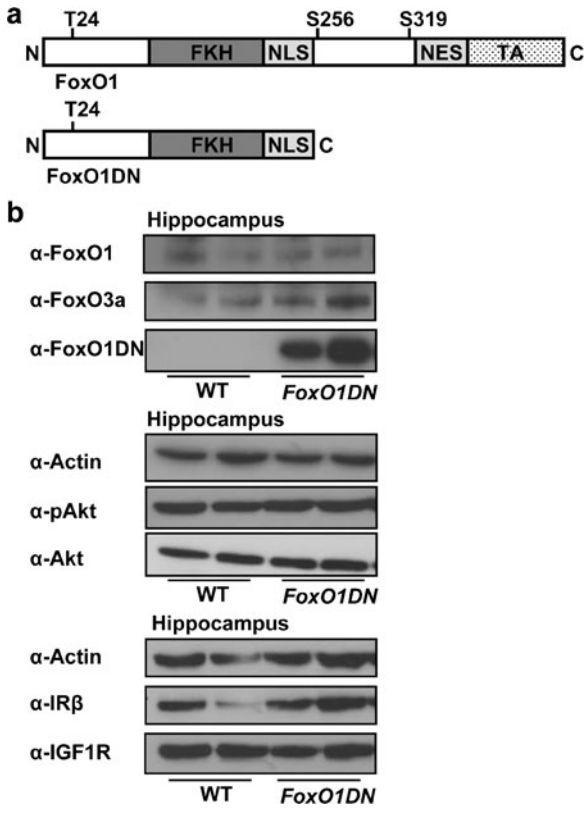

Fig. 7 *FoxO1DN* construct and conformation of transgene expression. **a** *Upper panel* Wild type (WT) FoxO1 consisting of the forkhead binding domain (FKH), nuclear localization signal (NLS), nuclear exclusion signal (NES), and a C-terminal transactivation domain (TA). WT FoxO1 contains three Akt phosphorylation sites (Thr24, Ser256, and Ser319). *Lower panel* Schematic drawing of mutant FoxO1 (*FoxO1DN*). **b** Western blot analysis of hippocampal lysates of adult *FoxO1DN* and WT mice using antibodies against FoxO1, FoxO3a, IRβ, IGF1R, phospho-Akt (Ser473), and Akt. Actin served as loading control. Individual bands of the Western blots represent individual animals (3 independent experiments). *FoxO1* Forkhead box O protein 1, *FoxO3a* Forkhead box O protein 3a, *IRβ* beta subunit of insulin receptor, *IGF1R* insulinlike growth factor 1 receptor, *Akt* protein kinase B

used the same SynCre line as described above and analyzed male *FoxO1DN* mice at 60 weeks of age.

To detect FoxO1DN expression or possible compensations via FoxO1, FoxO3a, or alterations of the IR/IGF1R signaling cascade, we used WB of hippocampal lysates. As expected, FoxO1DN was only present in the corresponding genotype (*FoxO1DN*) (Fig. 7b). Furthermore, we could not detect any changes in wild type FoxO1 or FoxO3a expression (Fig. 7b). Similarly, IR and IGF1R as well as Akt abundance was unchanged in *FoxO1DN* compared to WT littermates. Moreover, Akt phosphorylation at Ser473 was unchanged as well (Fig. 7b).

Interestingly, fat mass (Fig. 8a), leptin levels (data not shown), growth (Fig. 8b,c), food and water intake (Fig. 8d, e) as well as circadian pattern of activity (Fig. 8f) were unchanged in these mice. In contrast to n*IRS2*^{tg} mice, *FoxO1DN* males showed a tendency to increased activity and EE (data not shown). Moreover, GTTs, ITTs, and measurements of random-fed and starved glucose levels revealed no differences between *FoxO1DN* and WT mice (data not shown). Thus, the phenotype of n*IRS2*^{tg} males is not related to decreased FoxO1-mediated transcription. Furthermore, exploratory behavior (Fig. 8g) or motor coordination (Fig. 8h) was unaltered in *FoxO1DN* mice.

Discussion

In the present study, we show that neuron-specific overexpression of IRS2 causes decreased voluntary locomotor activity leading to increased fat mass, insulin resistance, and glucose intolerance during aging. In the past decade, neuronal insulin or IGF1 signaling has been proposed as a therapeutic target for several conditions including AD and obesity. Recently, human trials up to a length of 6 months have shown efficacy of intranasal insulin administration (reaching the CSF without lowering blood glucose concentrations) to improve memory in AD patients and to reduce fat mass in men (Craft et al. 2012; Hallschmid et al. 2004). These trials led to an optimistic view of long-term use of insulin or insulinlike peptides. However, animal experiments addressing certain aspects of IR or IGF1R signaling have shown less optimistic results and raised safety concerns (Cohen et al. 2009; Freude et al. 2009a, b; Irvine et al. 2011; Killick et al. 2009; Sadagurski et al. 2011; Stohr et al. 2011a, b). Recently, several studies suggested an important role of central IRS2 signaling in regulating energy homeostasis (Burks et al. 2000; Choudhury et al. 2005; Withers et al. 1999), lifespan (Taguchi et al. 2007) and in the pathogenesis of neurodegenerative diseases (Freude et al. 2009a, b; Sadagurski et al. 2011).

However, up to now, there are no studies available exploring the effects of chronically increased IRS2-mediated signaling in neurons. Data obtained from mice harboring an *IRS2* deletion in all brain cells (including neurons, astrocytes, and oligodendrocytes) have revealed new insights into the function of central IRS2 signaling (Taguchi et al. 2007). In particular, brain-specific *IRS2* knockout (b*IRS2*$^{-/-}$) mice generated using the NesCre line are long-lived but insulin-resistant and hyperphagic (Taguchi et al. 2007). Furthermore, brain-specific *IRS2* deleted mice have increased spatial working memory (Irvine et al. 2011), suggesting that increased IRS2 signaling might, at least, partially be harmful. Hence, we generated a transgenic mouse model overexpressing IRS2 specifically in neurons. In neurons, chronically increased insulin signaling leads finally to insulin resistance (Kim et al. 2011). However, we did observe compensatory reduced IR, IGF1R, and IRS1 expression in n*IRS2*^{tg} mice, but we could also demonstrate that overexpression of IRS2 in the CNS in vivo leads to increased IRS2-mediated signaling. Thus, even though partially compensated, we generated a mouse model with chronically increased IRS2-mediated signals.

In contrast to previous studies, we did not use the NesCre line that expresses Cre-recombinase in the neuroepithelium leading to the target gene deletion in all brain cells. The SynCre line used in the present study is expressed only in postmitotic neurons (Zhu et al. 2001). This approach had the advantage that n*IRS2*^{tg} mice have no developmental malformation as has been described for b*IRS2*$^{-/-}$ mice using the NesCre line (microcephalus) (Taguchi et al. 2007). In fact, histopathological investigation of our n*IRS2*^{tg} mice proved unaltered brain development and structure. Thus, unlike previous studies, we were able to investigate the function of neuronal IRS2-mediated signals without any underlying developmental phenotype.

n*IRS2*^{tg} mice are fertile, have normal litter size, and show normal growth and postnatal development. Interestingly, n*IRS2*^{tg} mice showed slightly more pronounced waist; therefore, we measured body composition using NMR revealing increased fat mass in the

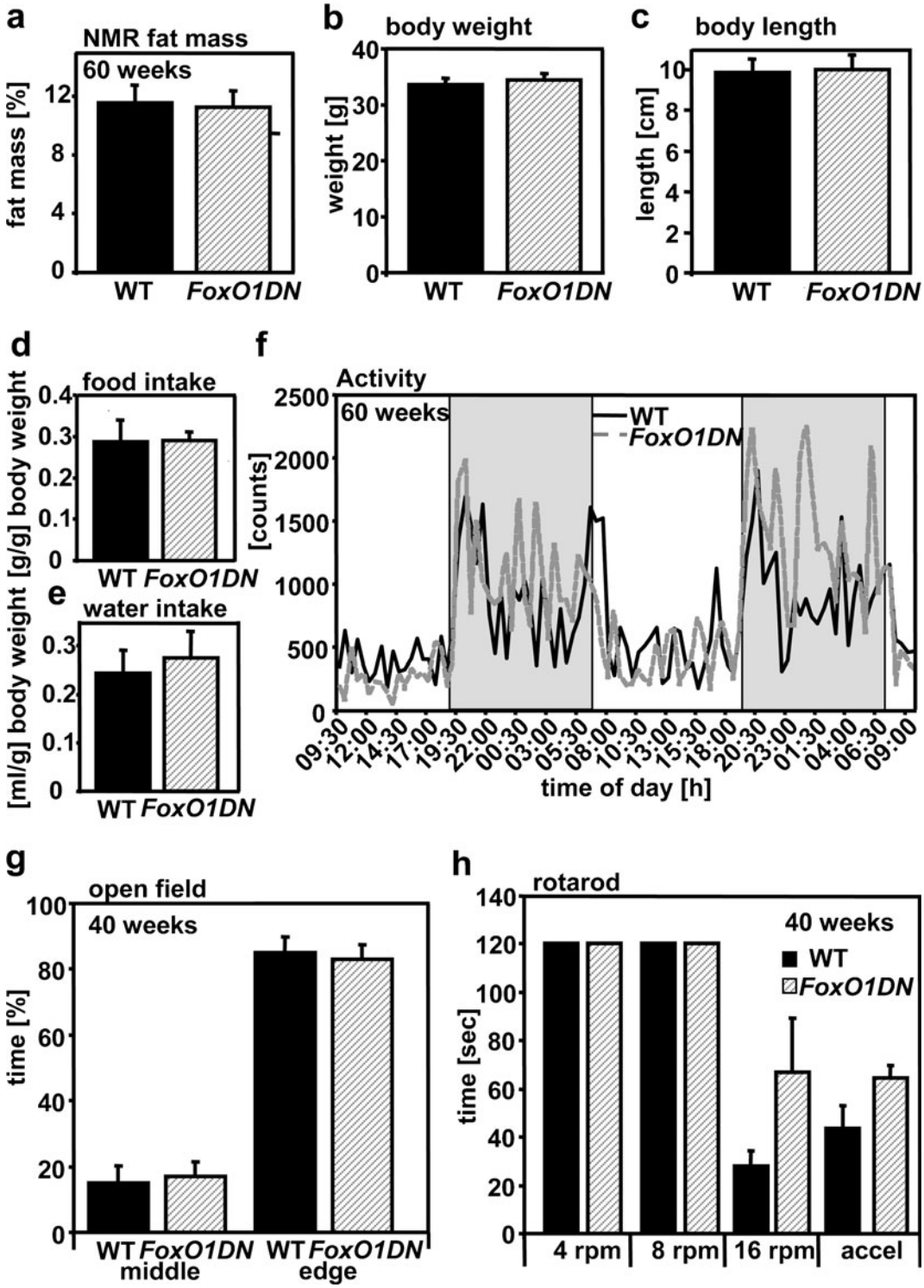

Fig. 8 Characterization of male *FoxO1DN* mice and respective controls. **a** Fat mass measured by nuclear magnetic resonance (NMR). **b**–**c** Body weight and length. **d**–**e** Food and water intake per gram of body weight. **f** Voluntary locomotor activity and circadian pattern. **g** Open field test. **h** Rotarod test, accel: latency to fall [s] at constantly increasing rounds per minute (rpm). Data are expressed as means ± SEM, $n=6$ per group, $^{*}p<0.05$ (Student's t test); **a**–**f**: age 60 weeks; **g**–**h**: age 40 weeks

male n*IRS2*^{tg} mice compared to WT males. In order to elucidate the pathophysiological basis for this phenotype, we comprehensively analyzed energy metabolism in these mice. Since decreased central IRS2 signaling has been shown to increase food intake (Burks et al. 2000; Taguchi et al. 2007), we determined food and water consumption. However, we did not observe any differences between the genotypes. Consequently, we measured voluntary locomotor activity and EE. Interestingly, mice presented with decreased locomotor activity and decreased EE during the dark phase. The extent of EE reduction was according to the decrease of voluntary activity. We could exclude alterations in exploratory behavior and motor coordination as contributing factors. Thus, we conclude that decreased spontaneous locomotor activity might be the basis for the observed increased fat mass as it has been shown for other mouse mutants (Mesaros et al. 2008). In line with this observation are data reported from mice being neuron specifically haplosufficient for the IGF1R. n*IGF-1R*$^{+/-}$ mice are slightly IGF1-resistant in neurons but show decreased fat accumulation during aging due to increased locomotor activity (Freude et al. 2012). Consistently, it has been reported that b*IRS2*$^{-/-}$ mice show nearly twice as much locomotor activity during aging (Taguchi et al. 2007). Since these mice are hyperphagic, the effect of increased physical activity might be counteracted by increased food intake. Taken together, the data presented here show that neuronal IRS2-mediated signals modulate voluntary locomotor activity.

In a second step, we investigated whether the decreased activity and increased fat mass had metabolic consequences during aging. Interestingly, male n*IRS2*^{tg} mice developed insulin resistance and glucose intolerance at the age of 100 weeks. Thus, chronically increased IRS2-mediated signals lead to insulin resistance via decreased physical activity. Hence, we identified neuronal IGF1R→IRS2-mediated signals as a relevant metabolic regulator for voluntary locomotor activity (model in Fig. 9). Interestingly, IRS1 deletion had no effect on locomotor activity (Stöhr O and Schubert M, unpublished data).

Recently, increased spatial working memory has been demonstrated in b*IRS2*$^{-/-}$ mice. In order to elucidate whether increased IRS2 signaling is indeed a negative regulator of memory formation (Irvine et al. 2011), we tested our animals for spontaneous alteration in the T-maze task. This task is not altered by decreased locomotor activity as, for example, the Morris Water Maze. However, we did not observe any differences in young (20 weeks) and old animals (100 weeks). Hence, we suggest that the increased spatial memory formation observed in b*IRS2*$^{-/-}$ mice might be due to a compensatory phenomenon and not directly related to IRS2 signaling. However, it is unclear why metabolic consequences of central manipulation of the IR/IGF1R signaling cascade in our mouse models only occur during aging (Freude et al. 2012; Kappeler et al. 2008).

IRS2-mediated signaling downregulates FoxO1-mediated transcription via phosphorylation of Akt, which, in turn, triggers nuclear exclusion and degradation of the FoxO transcription factors. Hence, we speculated that decreased FoxO-mediated transcription might be the molecular basis of the n*IRS2*^{tg} phenotype.

There are four different members of the mammalian FoxO family known: FoxO1, FoxO3a, FoxO4, and FoxO6. Apart from FoxO6, which is exclusively expressed in the brain (Jacobs et al. 2003; Zemva

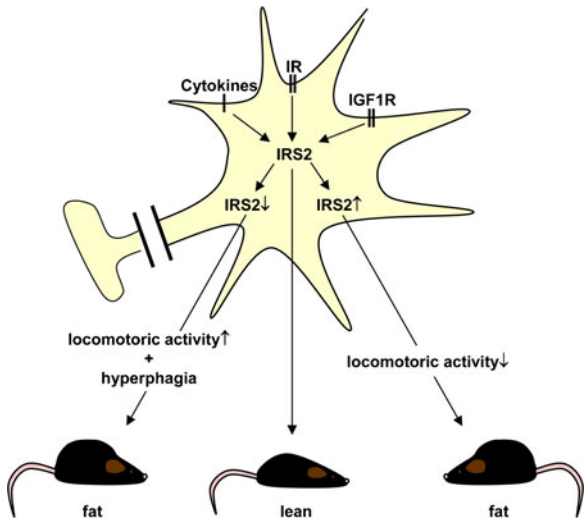

Fig. 9 Balanced central IGF1→IRS2 signaling is required for normal energy homeostasis. Integrating the present study with previously published data suggests a model where neuronal IGF1R→IRS2 signaling regulates voluntary locomotor activity in rodents. Decreased neuronal IRS2 signaling leads to hyperphagia and increased locomotoric activity overall resulting in age-associated insulin resistance and obesity. Chronically increased IRS2-mediated signals decrease locomotoric activity resulting in increased fat mass and age-associated insulin resistance as well. *IR* insulin receptor, *IGF1R* insulinlike growth factor 1 receptor, *IRS2* insulin receptor substrate 2

and Schubert 2011; Zemva et al. 2012), and FoxO4, which is not expressed in the CNS, FoxO transcription factors are found ubiquitously (Burgering 2008). mRNA expression data suggest that FoxO1 and FoxO3a are the major FoxOs in the murine brain. Because of the shared DNA-binding domain, FoxOs are expected to bind to similar DNA sequences and a core consensus sequence for FoxO-binding has been determined (5′-TTGTTTAC-3′) (Furuyama et al. 2000). Thus, all FoxOs hypothetically regulate the same set of genes through binding to this sequence. Functional specificity is likely to be achieved via interaction with coregulators or via differential expression (Burgering 2008). Several groups have successfully used a transactivation domain-deleted FoxO1 mutant to suppress FoxO-induced transcription (Kitamura et al. 2007). Therefore, we generated mice expressing the FoxO1DN mutant in exactly the same set of neurons as the transgene of n*IRS2*^{tg} mice. However, comprehensive analysis of these mice did not reveal any of the phenotypes observed in n*IRS2*^{tg} mice. Thus, FoxO1 is most likely not involved in the modulation of locomotor activity mediated via IRS2.

Integrating the present study into previously published data we conclude: (1) neuronal IRS2 signaling regulates voluntary locomotor activity at least in rodents. Chronically activated IRS2-mediated signals decrease, whereas permanently reduced IRS2 signaling increases locomotor activity. (2) Long-term decreased locomotor activity mediated via increased IRS2 expression might lead to increased fat mass, insulin resistance, and glucose intolerance during aging. (3) Neuron-specific IRS2 overexpression does not disturb spatial working memory. (4) The observed central IRS2-mediated effects are not dependent on reduced FoxO transcription. Thus, balanced IRS2 signaling in the CNS is required for normal energy homeostasis.

Acknowledgments This work was supported by AFI #08813. JZ was supported by a student's grant of the Medical Faculty, University of Cologne. We thank Andre Kleinridders for his kind introduction and troubleshooting in transgenic mouse generation. Also, we thank Thomas Wunderlich for kindly providing the pCAGGS targeting vector. Thanks also to Jens Alber for excellent technical assistance, Prof. Wilhelm Stoffel for providing the T-maze, and Prof. Martina Deckert and Mariana Carstov for advice and help on immunohistochemistry.

References

Brunet A, Bonni A, Zigmond MJ, Lin MZ, Juo P, Hu LS, Anderson MJ, Arden KC, Blenis J, Greenberg ME (1999) Akt promotes cell survival by phosphorylating and inhibiting a Forkhead transcription factor. Cell 96(6):857–868

Burgering BM (2008) A brief introduction to FOXOlogy. Oncogene 27(16):2258–2262

Burks DJ, Font de Mora J, Schubert M, Withers DJ, Myers MG, Towery HH, Altamuro SL, Flint CL, White MF (2000) IRS-2 pathways integrate female reproduction and energy homeostasis. Nature 407(6802):377–382

Cheng Z, White MF (2012) The AKTion in non-canonical insulin signaling. Nat Med 18(3):351–353

Cheng Z, Guo S, Copps K, Dong X, Kollipara R, Rodgers JT, Depinho RA, Puigserver P, White MF (2009) Foxo1 integrates insulin signaling with mitochondrial function in the liver. Nat Med 15(11):1307–1311

Chirivella L, Cano-Jaimez M, Perez-Sanchez F, Herraez L, Carretero J, Farinas I, Burks DJ, Kirstein M (2012) IRS2 signalling is required for the development of a subset of sensory spinal neurons. Eur J Neurosci 35 (3):341–352

Choudhury AI, Heffron H, Smith MA, Al-Qassab H, Xu AW, Selman C, Simmgen M, Clements M, Claret M, Maccoll G, Bedford DC, Hisadome K, Diakonov I, Moosajee V, Bell JD, Speakman JR, Batterham RL, Barsh GS, Ashford ML, Withers DJ (2005) The role of insulin receptor substrate 2 in hypothalamic and beta cell function. J Clin Invest 115 (4):940–950

Cohen E, Paulsson JF, Blinder P, Burstyn-Cohen T, Du D, Estepa G, Adame A, Pham HM, Holzenberger M, Kelly JW, Masliah E, Dillin A (2009) Reduced IGF-1 signaling delays age-associated proteotoxicity in mice. Cell 139 (6):1157–1169

Craft S, Baker LD, Montine TJ, Minoshima S, Watson GS, Claxton A, Arbuckle M, Callaghan M, Tsai E, Plymate SR, Green PS, Leverenz J, Cross D, Gerton B (2012) Intranasal insulin therapy for Alzheimer disease and amnestic mild cognitive impairment: a pilot clinical trial. Arch Neurol 69(1):29–38

Deacon RM, Rawlins JN (2006) T-maze alternation in the rodent. Nat Protoc 1(1):7–12

Dhamoon MS, Noble JM, Craft S (2009) Intranasal insulin improves cognition and modulates beta-amyloid in early AD. Neurology 72(3):292–293, author reply 293–4

Dong XC, Copps KD, Guo S, Li Y, Kollipara R, DePinho RA, White MF (2008) Inactivation of hepatic Foxo1 by insulin signaling is required for adaptive nutrient homeostasis and endocrine growth regulation. Cell Metab 8(1):65–76

Eggan K, Akutsu H, Loring J, Jackson-Grusby L, Klemm M, Rideout WM 3rd, Yanagimachi R, Jaenisch R (2001) Hybrid vigor, fetal overgrowth, and viability of mice derived by nuclear cloning and tetraploid embryo complementation. Proc Natl Acad Sci U S A 98(11):6209–6214

Freude S, Leeser U, Muller M, Hettich MM, Udelhoven M, Schilbach K, Tobe K, Kadowaki T, Kohler C, Schroder H, Krone W, Bruning JC, Schubert M (2008) IRS-2 branch of IGF-1 receptor signaling is essential for appropriate timing of myelination. J Neurochem 107(4):907–917

Freude S, Schilbach K, Schubert M (2009a) The role of IGF-1 receptor and insulin receptor signaling for the pathogenesis of Alzheimer's disease: from model organisms to human disease. Curr Alzheimer Res 6(3):213–223

Freude S, Hettich MM, Schumann C, Stohr O, Koch L, Kohler C, Udelhoven M, Leeser U, Muller M, Kubota N, Kadowaki T, Krone W, Schroder H, Bruning JC, Schubert M (2009b) Neuronal IGF-1 resistance reduces Abeta accumulation and protects against premature death in a model of Alzheimer's disease. FASEB J 23(10):3315–3324

Freude S, Schilbach K, Hettich MM, Bronneke HS, Zemva J, Krone W, Schubert M (2012) Neuron-specific deletion of a single copy of the insulin-like growth factor-1 receptor gene reduces fat accumulation during aging. Horm Metab Res 44(2):99–104

Furuyama T, Nakazawa T, Nakano I, Mori N (2000) Identification of the differential distribution patterns of mRNAs and consensus binding sequences for mouse DAF-16 homologues. Biochem J 349(Pt 2):629–634

Hallschmid M, Benedict C, Schultes B, Fehm HL, Born J, Kern W (2004) Intranasal insulin reduces body fat in men but not in women. Diabetes 53(11):3024–3029

He XP, Kotloski R, Nef S, Luikart BW, Parada LF, McNamara JO (2004) Conditional deletion of TrkB but not BDNF prevents epileptogenesis in the kindling model. Neuron 43(1):31–42

Irvine EE, Drinkwater L, Radwanska K, Al-Qassab H, Smith MA, O'Brien M, Kielar C, Choudhury AI, Krauss S, Cooper JD, Withers DJ, Giese KP (2011) Insulin receptor substrate 2 is a negative regulator of memory formation. Learn Mem 18(6):375–383

Jacobs FM, van der Heide LP, Wijchers PJ, Burbach JP, Hoekman MF, Smidt MP (2003) FoxO6, a novel member of the FoxO class of transcription factors with distinct shuttling dynamics. J Biol Chem 278(38):35959–35967

Kappeler L, De Magalhaes FC, Dupont J, Leneuve P, Cervera P, Perin L, Loudes C, Blaise A, Klein R, Epelbaum J, Le Bouc Y, Holzenberger M (2008) Brain IGF-1 receptors control mammalian growth and lifespan through a neuroendocrine mechanism. PLoS Biol 6(10):e254

Killick R, Scales G, Leroy K, Causevic M, Hooper C, Irvine EE, Choudhury AI, Drinkwater L, Kerr F, Al-Qassab H, Stephenson J, Yilmaz Z, Giese KP, Brion JP, Withers DJ, Lovestone S (2009) Deletion of Irs2 reduces amyloid deposition and rescues behavioural deficits in APP transgenic mice. Biochem Biophys Res Commun 386(1):257–262

Kim B, McLean LL, Philip SS, Feldman EL (2011) Hyperinsulinemia induces insulin resistance in dorsal root ganglion neurons. Endocrinology 152(10):3638–3647

Kitamura T, Kitamura YI, Funahashi Y, Shawber CJ, Castrillon DH, Kollipara R, DePinho RA, Kitajewski J, Accili D (2007) A Foxo/Notch pathway controls myogenic differentiation and fiber type specification. J Clin Invest 117 (9):2477–2485

Konner AC, Hess S, Tovar S, Mesaros A, Sanchez-Lasheras C, Evers N, Verhagen LA, Bronneke HS, Kleinridders A, Hampel B, Kloppenburg P, Bruning JC (2011) Role for insulin signaling in catecholaminergic neurons in control of energy homeostasis. Cell Metab 13(6):720–728

Kuhn R, Torres RM (2002) Cre/loxP recombination system and gene targeting. Methods Mol Biol 180:175–204

Lavan BE, Lane WS, Lienhard GE (1997a) The 60-kDa phosphotyrosine protein in insulin-treated adipocytes is a new member of the insulin receptor substrate family. J Biol Chem 272(17):11439–11443

Lavan BE, Fantin VR, Chang ET, Lane WS, Keller SR, Lienhard GE (1997b) A novel 160-kDa phosphotyrosine protein in insulin-treated embryonic kidney cells is a new member of the insulin receptor substrate family. J Biol Chem 272 (34):21403–21407

Mao X, Fujiwara Y, Orkin SH (1999) Improved reporter strain for monitoring Cre recombinase-mediated DNA excisions in mice. Proc Natl Acad Sci U S A 96(9):5037–5042

Mesaros A, Koralov SB, Rother E, Wunderlich FT, Ernst MB, Barsh GS, Rajewsky K, Bruning JC (2008) Activation of Stat3 signaling in AgRP neurons promotes locomotor activity. Cell Metab 7(3):236–248

Moloney AM, Griffin RJ, Timmons S, O'Connor R, Ravid R, O'Neill C (2010) Defects in IGF-1 receptor, insulin receptor and IRS-1/2 in Alzheimer's disease indicate possible resistance to IGF-1 and insulin signalling. Neurobiol Aging 31(2):224–243

Sadagurski M, Cheng Z, Rozzo A, Palazzolo I, Kelley GR, Dong X, Krainc D, White MF (2011) IRS2 increases mitochondrial dysfunction and oxidative stress in a mouse model of Huntington disease. J Clin Invest 121(10):4070–4081

Saltiel AR, Kahn CR (2001) Insulin signalling and the regulation of glucose and lipid metabolism. Nature 414 (6865):799–806

Schubert M, Brazil DP, Burks DJ, Kushner JA, Ye J, Flint CL, Farhang-Fallah J, Dikkes P, Warot XM, Rio C, Corfas G, White MF (2003) Insulin receptor substrate-2 deficiency impairs brain growth and promotes tau phosphorylation. J Neurosci 23(18):7084–7092

Selman C, Lingard S, Gems D, Partridge L, Withers DJ (2008) Comment on "Brain IRS2 signaling coordinates life span and nutrient homeostasis". Science 320(5879):1012, author reply 1012

Stohr O, Hahn J, Moll L, Leeser U, Freude S, Bernard C, Schilbach K, Markl A, Udelhoven M, Krone W, Schubert M (2011a) Insulin receptor substrate-1 and −2 mediate resistance to glucose-induced caspase-3 activation in human neuroblastoma cells. Biochim Biophys Acta 1812 (5):573–580

Stohr O, Schilbach K, Moll L, Hettich MM, Freude S, Wunderlich FT, Ernst M, Zemva J, Bruning JC, Krone W, Udelhoven M, Schubert M (2011b) Insulin receptor signaling mediates APP processing and beta-amyloid accumulation without altering survival in a transgenic mouse model of Alzheimer's disease. Age (Dordr)

Sun XJ, Rothenberg P, Kahn CR, Backer JM, Araki E, Wilden PA, Cahill DA, Goldstein BJ, White MF (1991) Structure of the insulin receptor substrate IRS-1 defines a unique signal transduction protein. Nature 352(6330):73–77

Sun XJ, Wang LM, Zhang Y, Yenush L, Myers MG Jr, Glasheen E, Lane WS, Pierce JH, White MF (1995) Role of IRS-2 in insulin and cytokine signalling. Nature 377(6545):173–177

Taguchi A, Wartschow LM, White MF (2007) Brain IRS2 signaling coordinates life span and nutrient homeostasis. Science 317(5836):369–372

Tschop MH, Speakman JR, Arch JR, Auwerx J, Bruning JC, Chan L, Eckel RH, Farese RV Jr, Galgani JE, Hambly C, Herman MA, Horvath TL, Kahn BB, Kozma SC, Maratos-Flier E, Muller TD, Munzberg H, Pfluger PT, Plum L, Reitman ML, Rahmouni K, Shulman GI, Thomas G, Kahn CR, Ravussin E (2012) A guide to analysis of mouse energy metabolism. Nat Methods 9(1):57–63

Udelhoven M, Pasieka M, Leeser U, Krone W, Schubert M (2010a) Neuronal insulin receptor substrate 2 (IRS2) expression is regulated by ZBP89 and SP1 binding to the IRS2 promoter. J Endocrinol 204(2):199–208

Udelhoven M, Leeser U, Freude S, Hettich MM, Laudes M, Schnitker J, Krone W, Schubert M (2010b) Identification of a region in the human IRS2 promoter essential for stress induced transcription depending on SP1, NFI binding and ERK activation in HepG2 cells. J Mol Endocrinol 44 (2):99–113

White MF (2003) Insulin signaling in health and disease. Science 302(5651):1710–1711

Withers DJ, Burks DJ, Towery HH, Altamuro SL, Flint CL, White MF (1999) Irs-2 coordinates Igf-1 receptor-mediated beta-cell development and peripheral insulin signalling. Nat Genet 23(1):32–40

Yamada M, Ohnishi H, Sano S, Nakatani A, Ikeuchi T, Hatanaka H (1997) Insulin receptor substrate (IRS)-1 and IRS-2 are tyrosine-phosphorylated and associated with phosphatidylinositol 3-kinase in response to brain-derived neurotrophic factor in cultured cerebral cortical neurons. J Biol Chem 272(48):30334–30339

Yenush L, White MF (1997) The IRS-signalling system during insulin and cytokine action. Bioessays 19(6):491–500

Zemva J, Schubert M (2011) Central insulin and insulin-like growth factor-1 signaling—implications for diabetes associated dementia. Curr Diabetes Rev 7(5):356–366

Zemva J, Schilbach K, Stöhr O, Moll L, Franko A, Krone W, Wiesner RJ and Schubert M (2012) Central FoxO3a and FoxO6 expression is down regulated in obesity induced diabetes but not in aging. Exp Clin Endocrinol Diabetes 120(6):340–350

Zhu Y, Romero MI, Ghosh P, Ye Z, Charnay P, Rushing EJ, Marth JD, Parada LF (2001) Ablation of NF1 function in neurons induces abnormal development of cerebral cortex and reactive gliosis in the brain. Genes Dev 15(7):859–876